

Identification of Hydrophobic Residues Critical for DPP-IV Dimerization[†]Chia-Hui Chien,[‡] Chia-Hua Tsai,[‡] Chun-Hung Lin,[§] Chi-Yuan Chou,^{||} and Xin Chen^{*,‡}

Division of Biotechnology and Pharmaceutical Research, National Health Research Institutes, Miaoli 350,
Institute of Biological Chemistry, Academia Sinica, Taipei 115, and Faculty of Life Science,
National Yang-Ming University, Taipei 112, Taiwan, ROC

Received February 28, 2006; Revised Manuscript Received April 10, 2006

ABSTRACT: The prolyl dipeptidase DPP-IV plays diverse and important roles in cellular functions. It is a membrane-bound exoprotease involved in the proteolytic cleavage of several insulin-sensing hormones. The inhibition of its enzymatic activity has been proven effective in the treatment of type II diabetes. Homodimeric DPP-IV interacts extracellularly with adenosine deaminase, and this interaction is critical for adenosine signaling and T-cell proliferation. In this study, we investigated the contribution of hydrophobic interactions to the dimerization of DPP-IV. Hydrophobic residues F713, W734, and Y735 were found to be essential for DPP-IV dimerization. Moreover, the enzymatic activity of DPP-IV was correlated with its quaternary structure. Monomeric DPP-IV had only residual activity left, ranging from 1/30 to 1/1600 of the dimeric forms. Using a surface plasmon resonance technique, we demonstrated that the affinity of these DPP-IV monomers for adenosine deaminase was not significantly altered, compared to that of dimeric DPP-IV. The study not only identifies the hydrophobic interactions critical for DPP-IV dimer formation, but also reveals no global conformational change upon the formation of monomers as determined by the protein–protein interaction (K_d) of DPP-IV with adenosine deaminase.

Dipeptidyl peptidase IV (DPP-IV¹, also known as CD26; EC 3.4.14.5) is a well-documented drug target in the treatment of type II diabetes. It belongs to the prolyl dipeptidase family, which includes DPP-IV, DPP8, DPP9, DPP2, and the fibroblast activation protein (FAP) (1, 2). These proteases preferentially cleave the peptide bond after the penultimate proline residue (1). DPP-IV, FAP, and DPP2 have proline-cleaving activities not normally possessed by other cellular proteases, which are important in their various biological functions in vivo (1). Determining the structure and regulation of DPP-IV should help to elucidate not only its function in vivo but also those of other homologous prolyl dipeptidases.

DPP-IV is a membrane-bound exoprotease with a 22-amino acid hydrophobic transmembrane region and a cytoplasmic tail of only six amino acids at the N-terminus. The structure of DPP-IV is homodimeric (3–6) (Figure 1A). Each

monomer of DPP-IV consists of an α/β hydrolase domain and a β -propeller domain, with the active site located between them (3–6). Two loops located at the dimer interface of DPP-IV are thought to be involved in the dimeric interaction: the C-terminal loop in the α/β hydrolase domain and the propeller loop that extends from strand 2 of the fourth blade in the β -propeller domain (3–5) (Figure 1A). The C-terminal loop, which consists of the last 50 amino acids in DPP-IV, has two α -helices (amino acids 713–725 and 745–763) and one β -sheet (amino acids 726–744) (3–5) (Figure 1B and C). It interacts with the same region of the other monomer across a 2-fold axis (Figure 1B). This loop is highly conserved among the prolyl dipeptidases (DPP-IV, FAP, DPP8, and DPP9) and the ion-channel proteins DPP6 and DPP10 (1) (Figure 1C). DPP6 and DPP10 lack enzymatic activity because of a mutation in the catalytic triad (7–10). Interestingly, the crystal structures of both FAP and DPPX are also homodimeric (11, 12). Their structures are highly superimposable on that of DPP-IV with similar dimer interfaces (11, 12). Identifying the residues important for DPP-IV dimer formation and maintenance should also elucidate DPP8 and DPP9, the structures and functions of which are yet to be determined.

DPP-IV plays diverse and important roles in cellular functions. It is involved in regulating the in vivo concentrations of two insulin-sensing hormones, glucagon-like peptide 1 (GLP-1) and glucose-dependent insulinotropic polypeptide (GIP) (13–15). Apart from the functional importance of its enzymatic activity, the interaction between DPP-IV and adenosine deaminase (ADA) is critical in the regulation of

[†] This study was financially supported by the National Health Research Institutes (grant BPR-094-PP-15 to X.C.), and the NRPGM, National Science Council (grant NSC95-3112-B-400-010 to X.C.), Taiwan, ROC.

* Corresponding author. Tel: 886-37-246166 ext 35718. Fax: 886-37-586456. E-mail: xchen@nhri.org.tw.

[‡] National Health Research Institutes.

[§] Academia Sinica.

^{||} National Yang-Ming University.

¹ Abbreviations: DPP-IV, dipeptidyl peptidase IV; rDPP-IV, human recombinant DPP-IV protein; DPP, dipeptidyl peptidase; H-Gly-Pro-pNA, H-Gly-Pro-p-nitroanilide; DTT, dithiothreitol; AUC, analytical ultracentrifugation; GLP-1, glucagon-like peptide-1; GIP, glucose-dependent insulinotropic polypeptide; FAP, fibroblast activation protein; ADA, adenosine deaminase; SPR, surface plasmon resonance.

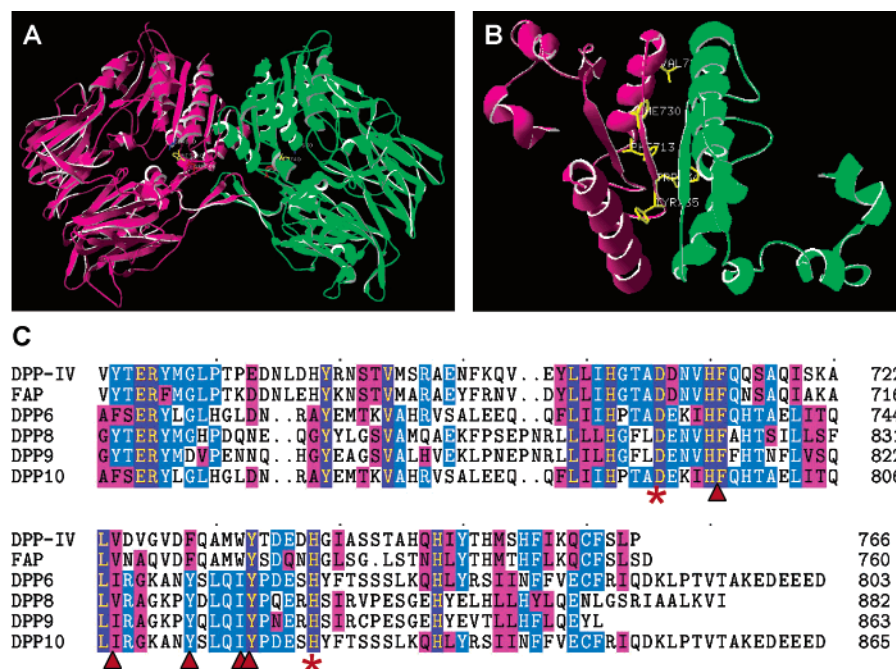


FIGURE 1: Location of the mutated hydrophobic residues of the C-terminal loop at the dimer interface. DPP-IV is homodimeric, illustrated with purple and green. Panel A: dimeric DPP-IV with the catalytic triad marked in yellow (Ser630), red (Asp708), and blue (His740). Panel B: enlarged view of the C-terminal loop with mutated hydrophobic residues F713, V724, F730, W734, and Y735. Panel C: alignment of the C-terminal loop of the DPP family. The mutated hydrophobic residues are marked below with red triangles, and the catalytic triad residues (Asp708 and His740) are marked with red stars. Panels A and B were drawn with the DeepView program version 3.7 (www.expasy.org/spdbv) with the structure of DPP-IV (pdb 1N1M). The alignment in panel C was constructed using the Clustal W and TEXSHADE programs (<http://workbench.sdsc.edu>).

adenosine signaling and in potentiating T-cell proliferation, leading to a marked increase in the costimulatory signals in the immunological synapse (16–18). A high concentration of adenosine at the cell surface inhibits T-cell function (19). ADA is responsible for the deamination of adenosine and 2'-deoxyadenosine to inosine and 2'-deoxyinosine (20). As a result, the adenosine concentration is tightly regulated on the surface of the plasma membrane via ADA anchored by DPP-IV (19). This is a high-affinity interaction, with K_d values in the nanomolar range (21–25). A cocrystallization study demonstrated that ADA interacts with DPP-IV in a 1:1 ratio through the latter's propeller domain, opposite and distant from the dimerization interface (26). The interaction surface is highly amphipathic, involving both hydrophobic and hydrophilic interactions (26). Whether the dimeric structure of DPP-IV is essential for its interaction with ADA is unknown.

In this study, we investigated the contribution of hydrophobic interactions to DPP-IV dimerization using site-directed mutagenesis. The enzymatic activity of DPP-IV and its interaction with ADA were investigated with respect to its quaternary structure. The interaction of monomeric DPP-IV with ADA has not been explored previously, and our results reveal novel properties of monomeric DPP-IVs.

EXPERIMENTAL PROCEDURES

Materials. The enzyme substrate H-Gly-Pro-pNA was purchased from Bachem, Switzerland. Fetal bovine serum was from Hyclone. Lipofectin and insect culture media (Grace's medium and Express Five medium) were from Invitrogen. The human liver cDNA library and linear viral vector were from Clontech. The Western detection kit Western Lightning was from Perkin-Elmer. Q Sepharose

High Performance and CM5 chip were from Amersham-Pharmacia. Bovine adenosine deaminase (ADA) was from Roche.

Plasmid Construction. The baculovirus expression plasmid pBac8-CD5 encoding DPP-IV (amino acids 39–766) has been described previously (27). Site-directed mutagenesis of the gene for DPP-IV was performed as previously described (27). The primers used were 5'-gataacgttcacaggcagcagtcagc-3' and 5'-gctgactgctgctgtgaacgttacc-3' for F713A; 5'-caaagc-cctggccgatgttgag-3' and 5'-ctccaacatcgccagggtttg-3' for V724A; 5'-ggagtggatgccaggcaatg-3' and 5'-cattgctgggcatc-cactcc-3' for F730A; 5'-gcaatgtgggctactgatgaag-3' and 5'-cttcacatgtagccacattgc-3' for W734; and 5'-cttcacatgtagc-cacattgc-3' and 5'-gcaatgtgggctactgatgaag-3' for Y735A. All coding regions were sequenced to verify that they contained no mutations other than those intended.

Insect Cell Culture, DNA Transfection, Virus Selection, and Amplification. Sf9 cells were grown at 27 °C in Grace's medium supplemented with 10% fetal bovine serum. The transfection of DNA into Sf9 cells and the selection and amplification of the recombinant virus were performed as described previously (29). For expression and purification purposes, Hi5 cells were used instead of Sf9 cells. Hi5 cells were infected at a multiplicity of infection (MOI) of 1, determined previously to be the optimal condition for protein expression (28), and the cells were harvested 72 h after infection.

Purification and Characterization of the DPP-IV Protein. Recombinant DPP-IVs were purified on an ADA affinity column as described previously (27). The purified proteins were stored at –80 °C and used within one month. Freezing does not change either the quaternary structure (determined by analytical ultracentrifugation (AUC)) or the enzymatic

activities of DPP-IV proteins (data not shown). The purity of the proteins was determined by sodium dodecyl sulfate–polyacrylamide gel electrophoresis (SDS–PAGE), and the proteins were visualized with Coomassie Blue staining. The amount of protein was determined using bovine serum albumin as the standard (29). Gel filtration of the purified proteins was performed as described previously (27).

Determination of Kinetic Constants. The kinetic constants were determined as described previously, using the chromogenic substrate H-Gly-Pro-pNA (27). The reaction was monitored by the absorbance at 405 nm as a function of time. The enzyme concentrations used in the reaction were 10 nM for dimeric DPP-IVs, 100 nM for monomeric DPP-IVs including F713A, V724A, F730A, and W734A, and 500 nM for monomeric Y735A. The initial rate was measured with less than 10% substrate depletion for the first 10–300 s. The steady-state parameters, k_{cat} and K_m , were determined from initial velocity measurements at 0.5–5 K_m of the substrate concentrations. The kinetic parameters were analyzed using nonlinear regression of the Michaelis–Menten equation. Correlation coefficients greater than 0.99 were obtained throughout.

Analytical Ultracentrifugation. An AUC analysis of the purified DPP-IV proteins was performed as described previously at concentrations of about 0.1–0.2 mg/mL (1.2–2.3 μM) (27). The sedimentation coefficients (S) of the enzymes were estimated with a Beckman-Coulter XL-A analytical ultracentrifuge with an An60Ti rotor, as described previously (30). The sedimentation velocity experiment was performed at 40 000 rpm at 20 °C with a standard double-sector aluminum centerpiece. The UV absorption of the cells was measured every 10 min for 4 h. The sedimentation equilibrium experiment was performed at 20 °C with a six-channel centerpiece, with centrifugation at 12 000 rpm for 12 h. Both sets of data were analyzed with the program Sedfit version 9.2 (<http://www.analyticalultracentrifugation.com>) to calculate the molecular weights and sedimentation coefficients (30). The Sednterp version 1.07 program (<http://www.jphilo.mailway.com/>) was used to calculate solvent densities, viscosities, Stokes' radii (R_s), and anhydrous frictional ratios (f/f_0).

Surface Plasma Resonance (SPR) Technology. An SPR analysis of the binding of recombinant human DPP-IV to bovine ADA was performed with a BIAcore 2000 instrument (BIAcore, Uppsala, Sweden). Instead of immobilizing the DPP-IV as described previously (31), we immobilized bovine ADA (Roche) on a CM5 sensor chip, using the amine-coupling reagents *N*-hydroxysuccinimide and 1-ethyl-3-(3-dimethylaminopropyl)-carbodiimide provided by the manufacturer. Specifically, ADA was diluted with 10 mM sodium acetate (pH 4.5) to a final concentration of 0.5 mg/mL. It was immobilized on the control and sample chips at a flow rate of 20 $\mu\text{L}/\text{min}$, before it was blocked with ethanolamine. Generally, 4500–8800 response units (RU) were detected after immobilization. The interaction kinetics were determined at room temperature by injecting 90 μL of DPP-IV protein in phosphate-buffered saline (PBS) at a flow rate of 30 $\mu\text{L}/\text{min}$ for 3 min and then PBS only for 5 min to achieve dissociation. The concentration range of the DPP-IVs used in these experiments ranged in 2-fold serial dilutions from 1.5 μM to 94 nM. Typically, 80–230 RU of DPP-IV protein were detected bound to the chip-immobilized ADA. Ethylene

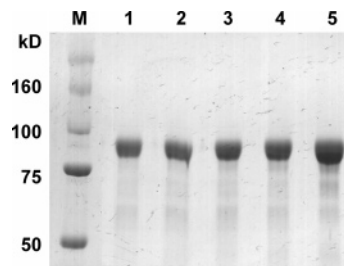


FIGURE 2: Purified recombinant DPP-IV proteins from baculovirus-infected insect cells. M: molecular weight markers. Lanes 1 to 5: F713A, V724A, F730A, W734A, and Y735A, respectively.

glycol (95.2%) was used as the regeneration agent at a flow rate of 20 $\mu\text{L}/\text{min}$ for 1 min before PBS was applied for at least 5 min as the stabilization buffer. Under these conditions, ADA was completely washed off because the signal returned to baseline. Under the conditions described, the chips are stable for repeated use (over 50 times). The BIAevaluation software provided by the manufacturer was used to analyze the data and to calculate k_{on} and k_{off} using a 1:1 interaction model.

RESULTS

Hydrophobic Interaction is Essential for DPP-IV Dimer Formation. Several hydrophobic residues in the C-terminal region of DPP-IV are conserved in the prolyl dipeptidase family (Figure 1C). The structural role of these residues in DPP-IV dimerization is an intriguing subject. We performed site-directed mutagenesis on the following hydrophobic residues: F713, V724, F730, W734, and Y735, on the basis of their conservation and their locations at the dimer interface (Figure 1B and C). Because recombinant DPP-IV proteases from baculovirus-infected insect cells have biochemical properties similar to those of endogenous DPP-IV (4, 27), we chose that expression system for this study. All mutant DPP-IV proteins were purified as shown in Figure 2.

Sedimentation velocity and sedimentation equilibrium, measured by AUC, were used to study the quaternary structure of DPP-IVs (Figure 3 and Table 1). Recombinant wild-type DPP-IV is dimeric, with a sedimentation coefficient of 8.4 S and a molecular weight of 187 (Figure 3A and Table 1). Single-site mutations at F713, W734, or Y735 (generating F713A, W734A, or Y735A, respectively) disrupted dimeric DPP-IV into monomers (Figure 3B, E, and F, respectively), with only a small fraction of dimers present in the W734A mutant. In contrast, V724A remained largely dimeric (Figure 3C), whereas F730A was a mixture of monomers and dimers (Figure 3D). The Stokes' radii ranged from 3.7 to 4.4 nm for monomeric DPP-IVs, and from 5.0 to 5.5 nm for dimers (Table 1). The sedimentation coefficients were around 5.1 S to 5.8 S for monomeric DPP-IVs, and 8.4 S for dimers (Table 1). The molecular weights determined were 187–195 for dimers and 89–97 for monomers (Table 1). The f/f_0 ratios were all greater than 1, indicating that no DPP-IV protein was spherical, whether monomeric or dimeric (Table 1). These results provide the first experimental evidence that hydrophobic interactions together with the hydrophilic interactions identified previously (27) are important for holding DPP-IV together in the dimeric form. Moreover, residues F713, W734, and Y735 provide critical and essential

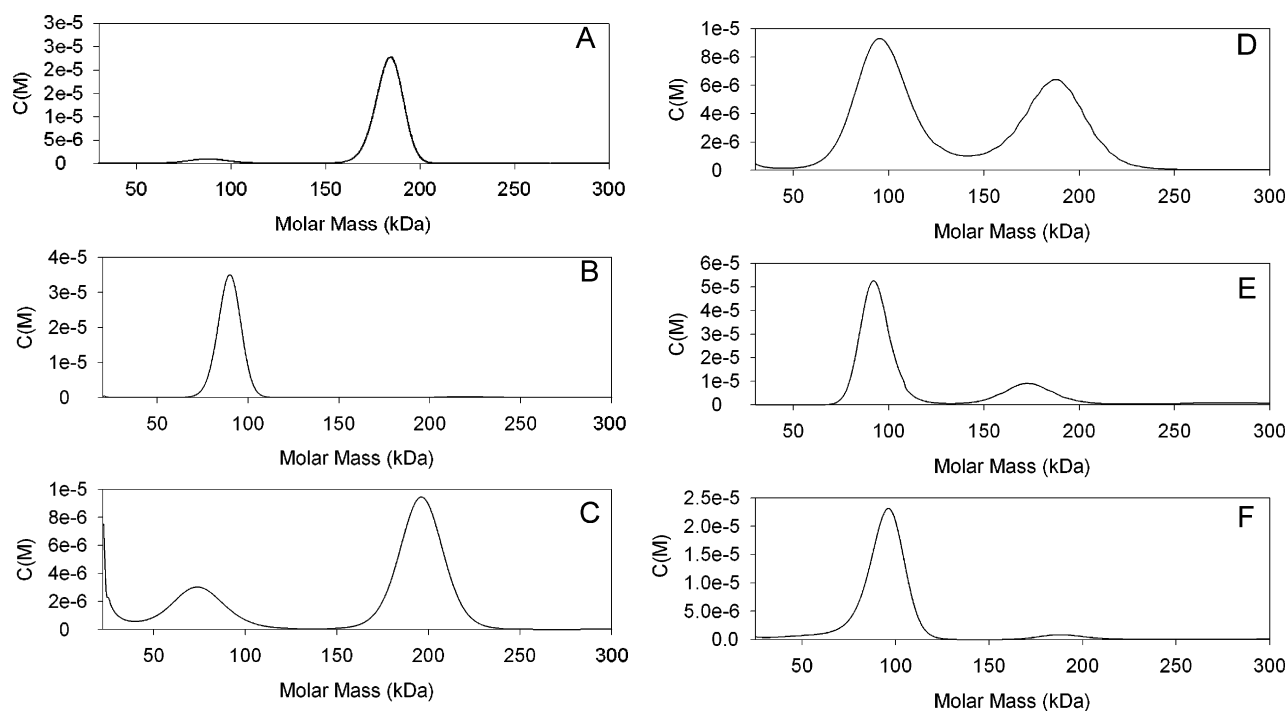


FIGURE 3: Sedimentation velocity analysis of DPP-IV proteins. Panels A–F: wild-type rDPP-IV, F713A, V724A, F730A, W734A, and Y735A, respectively. Each panel represents the sedimentation-coefficient distribution of all species.

Table 1: Hydrodynamic Properties of Wild-Type and Mutant DPP-IVs^a

	rDPP-IV	F713A	V724A		F730A		W734A	Y735A
quaternary structure	dimer	monomer	dimer	monomer	dimer	monomer	monomer	monomer
Stokes' radius (nm)	5.0	3.7	5.5	4.4	5.3	4.3	3.8	3.9
sedimentation coefficient (S)	8.4	5.7	8.4	5.1	8.4	5.3	5.6	5.8
molecular weight	187	89	195	97	188	95	91	97
anhydrous frictional ratio (f/f_0)	1.4	1.3	1.4	1.4	1.4	1.4	1.3	1.3

^a The experiments were repeated at least twice with similar results. One representative set of data is shown here. The predicted molecular weight of monomeric recombinant human DPP-IV without glycosylation is 84371.

interactions in the DPP-IV dimer, whereas V724 and F730 are much less important.

In a previous study, we found that once formed, dimeric and monomeric DPP-IVs do not equilibrate at all in solution (27). Consistent with this, we also found with AUC that the monomers and dimers of V724A and F730A do not equilibrate at all after they are separated by gel filtration (data not shown). These results suggest that regardless of the site of the DPP-IV mutation, the monomeric form of the protease adopts a conformation that is incapable of overcoming the energy barrier to form dimers in solution and vice versa.

Enzymatic Activity of DPP-IV Correlates with Its Quaternary Structure. To determine whether the enzymatic activity of DPP-IV correlates with its quaternary structure, we measured the enzymatic activities of DPP-IV after separating monomers from dimers by gel filtration chromatography as described in Experimental Procedures. As shown in Table 2, the enzymatic activities of DPP-IV correlated perfectly with its quaternary structure. The dimeric forms of the V724A and F730A proteins exhibited a decrease in activity, determined from k_{cat}/K_m values, of only 2-fold relative to that of wild-type dimeric DPP-IV (Table 2). However, all monomeric forms of DPP-IVs displayed only a fraction of residual activity, ranging from 1/30 (F713A) and 1/250 (monomers of V724A, F730A, and W734A) to

Table 2: Kinetic Constants of Wild-Type and Mutant DPP-IVs^a

	quaternary structure	k_{cat} (s ⁻¹)	K_m (μM)	k_{cat}/K_m (s ⁻¹ M ⁻¹)
rDPP-IV	dimer	87 ± 1.4	90 ± 2.1	967
F713A	monomer	1.8 ± 1.2	50 ± 1.5	36
V724A	dimer	48 ± 8.9	88 ± 1.3	545
	monomer	0.5 ± 0.03	76 ± 1.5	7
F730A	dimer	28 ± 2	56 ± 1.6	500
	monomer	0.2 ± 0.01	54 ± 5.2	4
W734A	monomer	0.3 ± 0.2	90 ± 0.4	3
Y735A	monomer	0.05 ± 0.02	89 ± 0.7	0.6

^a Data were calculated from at least three independent measurements with different batches of enzymes. The substrate used was H-Gly-Pro-pNA.

1/1600 (Y735A) of the wild-type activity. Notably, these decreases in enzymatic activity all resulted from a drop in the k_{cat} values, whereas the K_m values remained unchanged (Table 2). Therefore, the enzymatic activity of DPP-IV correlates with its quaternary structure, and the dimeric structure of DPP-IV is essential for optimal catalytic activity.

Interaction of DPP-IV with ADA Determined by SPR. Whether changes in the quaternary structure of DPP-IV affect its interaction with ADA has been unknown until now. We used SPR technology to measure the affinity between DPP-IV and ADA. Bovine ADA was used for the study because it shares 91% amino acid sequence homology with human

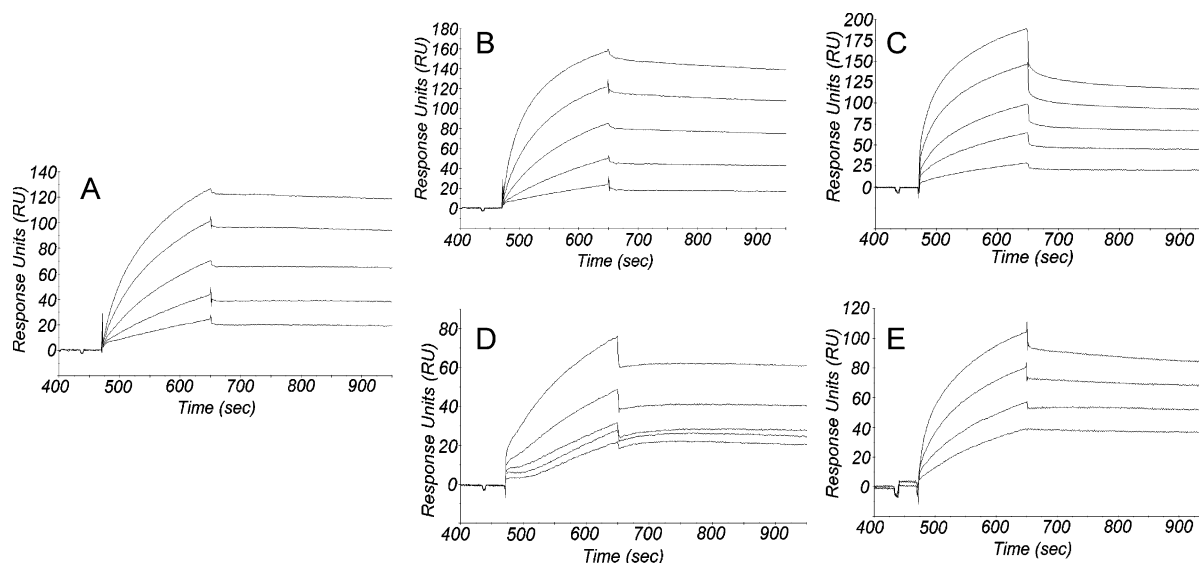


FIGURE 4: SPR sensorgrams used to determine the affinities of DPP-IV for ADA. Different concentrations of each DPP-IV, ranging from 1.5 μ M to 94 nM, were passed over chip-immobilized ADA to determine their kinetics of binding to ADA, as described in Experimental Procedures. Panels A–E: SPR sensorgrams to determine the affinities of dimeric rDPP-IV, monomeric forms of F713A, F730A, Y735A, and H750E, respectively, for ADA.

Table 3: Kinetics and Binding Affinities of Monomeric DPP-IVs for ADA^a

	k_{on} ($M^{-1} s^{-1}$)	k_{off} (s^{-1})	K_d (nM) ^b
rDPP-IV	$6.6 \pm 2.0 \times 10^3$	$7.1 \pm 2.3 \times 10^{-5}$	11
F713A monomer	$6.5 \pm 1.2 \times 10^3$	$3.2 \pm 0.9 \times 10^{-4}$	49
F730A monomer	$1.2 \pm 0.03 \times 10^4$	$2.0 \pm 0.7 \times 10^{-4}$	17
Y735A monomer	$1.4 \pm 0.05 \times 10^4$	$1.6 \pm 0.3 \times 10^{-4}$	12
H750E monomer	$5.6 \pm 1.1 \times 10^3$	$2.8 \pm 2.1 \times 10^{-4}$	50

^a The experiments were repeated using at least two different batches of the proteins. ^b K_d was calculated as k_{off}/k_{on} , where k_{off} and k_{on} are the association and dissociation rate constants, respectively.

ADA (26). As shown in Figure 4 and Table 3, wild-type human DPP-IV interacted with bovine ADA with a K_d value of 11 nM, similar to the values determined previously with either SPR and DPP-IV immobilized to a chip (5) or with direct-binding assays using ^{125}I -labeled bovine ADA and plasma membrane containing human DPP-IV (22, 32). Interestingly, monomeric DPP-IVs interacted with ADA with similar affinities, with K_d values ranging from 17 nM for F730A and 12 nM for F735A to 49 nM for F713A (Table 3). Monomeric H750E, generated by the disruption of the hydrophilic interaction (27), also interacted with ADA with a K_d value of 50 nM, similar to that of monomeric F713A (Table 3). Notably, the 5-fold differences in the K_d values for H750E and F713A resulted from decreases in the k_{off} values, whereas the k_{on} values remained the same as that of wild-type DPP-IV. These results indicate that changes in the quaternary structure of DPP-IV do not significantly affect its interaction with ADA.

DISCUSSION

DPP-IV is the first member of the prolyl dipeptidyl peptidase family whose biological function has been studied, its *in vivo* substrates identified, and its crystal structure resolved. Studying the regulation of the enzymatic activity of DPP-IV should extend our understanding of the biological functions and regulation of other homologous prolyl dipep-

tidases. In this study, the quaternary structure of DPP-IV was investigated with respect to its enzymatic activity and its interaction with ADA, and the hydrophobic residues important for DPP-IV dimer formation were identified.

Driven by crystallographic information and our previous study on the dimerization of DPP-IV (27), we chose five hydrophobic residues on the C-terminal loop that appear to be important in forming and maintaining the dimer interface and prepared single-site directed mutants of each residue. Three mutants (F713A, W734A, and Y735A) disrupt dimer formation, yielding monomers; V724A and F730A give mixtures of dimers and monomers by AUC. Significantly, we demonstrated that no interconversion of monomers and dimers was observed in either direction. This would suggest that dimer/monomer formation is an early committed step, perhaps at the level of protein folding. Once either species forms, it is highly stable and cannot easily retract to a form that permits an equilibrium between the two. It is also interesting that the mutant monomers are substantially less catalytically active than the corresponding mutant dimer and that the different is largely a k_{cat} effect. The location of the catalytic triad residues in and near the C-terminal loop is consistent with this observation and suggests that the monomer formation results in some catalytic misalignment that affects k_{cat} but not K_m . That the conformational differences of monomers and dimers are not global is supported by the similar binding of ADA to the wild type and mutants via the propeller domain of the protein. It shall be noted that these experiments were performed on soluble recombinant DPP-IV missing the N-terminal cytoplasmic tail and transmembrane domain (deletion of aa's 1–38). It is possible that the localization of native DPP-IV in the membrane might have a pronounced effect on the dimer/monomer results because the restricted degrees of freedom in the membrane might yield different results than with the soluble protein.

We have shown that monomeric DPP-IVs have affinities for ADA similar to that of wild-type dimeric DPP-IV (Table 3). In this study, we determined the affinity between dimeric human DPP-IV and bovine ADA to be 11 nM by SPR (Table

3), which is similar to the values obtained previously (12, 17, and 65 nM) using human DPP-IV and ^{125}I -labeled bovine ADA (21, 22, 32) or determined by SPR analysis of immobilized DPP-IV (3.2 nM) (5). This is also within the range of affinities measured previously (from 0.4 to 65 nM) with proteins obtained from different species (21, 22, 24, 31–33). However, we observed no significant difference in the affinities of the monomeric DPP-IVs for ADA compared to that of the dimeric DPP-IV, indicating that changes in the quaternary structure of DPP-IV have little impact on its propeller region, which interacts with ADA. The slightly lower affinities of F713A and H750E for ADA do not significantly affect the gross conformation of DPP-IV, as demonstrated by their similar K_m values and their amenability to purification on an ADA affinity column (Experimental Procedures). Importantly, we discovered that ethylene glycol was effective in removing bound DPP-IV from immobilized ADA in the SPR study. Because ethylene glycol is an effective reagent for the disruption of hydrophobic interactions, this observation corroborates the proposition that the main interaction between DPP-IV and ADA is hydrophobic (26, 31).

The optimal enzymatic activity of DPP-IV correlates with its dimeric structure. Hydrophobic residues F713, W734, and Y735 are essential for dimer formation and maintenance. F713 and W734 were previously shown in a crystallization study to locate at the dimer interface of porcine DPP-IV (3). The present results combined with those of a previous study (27) indicate that both hydrophobic and hydrophilic interactions (27) at the C-terminal loop contribute to the dimerization and optimal catalytic activity of DPP-IV. These different monomeric mutations might result in different intramolecular interactions. Indeed, we observed differential enzymatic activities (Table 2) and slightly different affinities for ADA among mutant DPP-IVs (Table 3). Further investigation of these monomers using crystallization studies should identify these subtle intramolecular changes. The hydrophobic residues identified in this study are conserved among different members of the DPP family, including DPP-IV, FAP, DPP8, DPP9, DPP6, and DPP10. Whether they play similar roles in other prolyl dipeptidases awaits further study.

ACKNOWLEDGMENT

We thank Mr. Robert Karlsson (BIAcore, Sweden) for suggestions and help on SPR analysis and Dr. Gu-Gang Chang for critically reading the manuscript and making suggestions. We thank Mr. Yuan-Shou Chen for his contribution to the mutagenesis of W734A and the 5F core facility of NHRI for using BIAcore2000.

REFERENCES

- Rosenblum, J. S., and Kozarich, J. W. (2003) Prolyl peptidases: a serine protease subfamily with high potential for drug discovery, *Curr. Opin. Chem. Biol.* 7, 496–504.
- Polgar, L. (2002) The prolyl oligopeptidase family, *Cell. Mol. Life Sci.* 59, 349–362.
- Engel, M., Hoffmann, T., Wagner, L., Wermann, M., Heiser, U., Kiefersauer, R., Huber, R., Bode, W., Demuth, H. U., and Brandstetter, H. (2003) The crystal structure of dipeptidyl peptidase IV (CD26) reveals its functional regulation and enzymatic mechanism, *Proc. Natl. Acad. Sci. U.S.A.* 100, 5063–5068.
- Rasmussen, H. B., Branner, S., Wiberg, F. C., and Wagtmann, N. (2003) Crystal structure of human dipeptidyl peptidase IV/CD26 in complex with a substrate analog, *Nat. Struct. Biol.* 10, 19–25.
- Thoma, R., Löffler, B., Stihle, M., Huber, W., Ruf, A., and Hennig, M. (2003) Structural basis of proline-specific exopeptidase activity as observed in human dipeptidyl peptidase-IV, *Structure* 11, 947–959.
- Fulop, V., Bocskei, Z., and Polgar, L. (1998) Prolyl oligopeptidase: an unusual beta-propeller domain regulates proteolysis, *Cell* 94, 161–170.
- Qi, S. Y., Riviere, P. J., Trojnar, J., Junien, J. L., and Akinsanya, K. O. (2003) Cloning and characterization of dipeptidyl peptidase 10, a new member of an emerging subgroup of serine proteases, *Biochem. J.* 373, 179–189.
- Wada, K., Yokotani, N., Hunter, C., Doi, K., Wenthold, R. J., and Shimasaki, S. (1992) Differential expression of two distinct forms of mRNA encoding members of a dipeptidyl aminopeptidase family, *Proc. Natl. Acad. Sci. U.S.A.* 89, 197–201.
- Zagha, E., Ozaita, A., Chang, S. Y., Nadal, M. S., Lin, U., Saganich, M. J., McCormack, T., Akinsanya, K. O., Qi, S. Y., and Rudy, B. (2005) DPP10 modulates Kv4-mediated A-type potassium channels, *J. Biol. Chem.* 280, 18853–18861.
- Nadal, M. S., Ozaita, A., Amarillo, Y., Vega-Saenz de Miera, E., Ma, Y., Mo, W., Goldberg, E. M., Misumi, Y., Ikehara, Y., Neubert, T. A., and Rudy, B. (2003) The CD26-related dipeptidyl aminopeptidase-like protein DPPX is a critical component of neuronal A-type K⁺ channels, *Neuron* 37, 449–461.
- Aertgeerts, K., Levin, I., Shi, L., Snell, G. P., Jennings, A., Prasad, G. S., Zhang, Y., Kraus, M. L., Salakian, S., Sridhar, V., Wijnands, R., and Tennant, M. G. (2005) Structural and kinetic analysis of the substrate specificity of human fibroblast activation protein alpha, *J. Biol. Chem.* 280, 19441–19444.
- Strop, P., Bankovich, A. J., Hansen, K. C., Garcia, K. C., and Brunger, A. T. (2004) Structure of a human A-type potassium channel interacting protein DPPX, a member of the dipeptidyl aminopeptidase family, *J. Mol. Biol.* 343, 1055–1065.
- Drucker, D. J. (2003) Therapeutic potential of dipeptidyl peptidase IV inhibitors for the treatment of type 2 diabetes, *Expert Opin. Invest. Drugs* 12, 87–100.
- Mentlein, R. (1999) Dipeptidyl-peptidase IV (CD26)—role in the inactivation of regulatory peptides, *Regul. Pept.* 85, 9–24.
- Pauly, R. P., Rosche, F., Wermann, M., McIntosh, C. H., Pederson, R. A., and Demuth, H. U. (1996) Investigation of glucose-dependent insulinotropic polypeptide-(1–42) and glucagon-like peptide-1-(7–36) degradation in vitro by dipeptidyl peptidase IV using matrix-assisted laser desorption/ionization-time-of-flight mass spectrometry. A novel kinetic approach, *J. Biol. Chem.* 271, 23222–23229.
- Dong, R. P., Tachibana, K., Hegen, M., Munakata, Y., Cho, D., Schlossman, S. F., and Morimoto, C. (1997) Determination of adenosine deaminase binding domain on CD26 and its immunoregulatory effect on T cell activation, *J. Immunol.* 159, 6070–6076.
- Dong, R. P., and Morimoto, C. (1996) Role of CD26 for CD4 memory T cell function and activation, *Hum. Cell* 9, 153–162.
- Pacheco, R., Martinez-Navio, J. M., Lejeune, M., Climent, N., Oliva, H., Gatell, J. M., Gallart, T., Mallol, J., Lluís, C., and Franco, R. (2005) CD26, adenosine deaminase, and adenosine receptors mediate costimulatory signals in the immunological synapse, *Proc. Natl. Acad. Sci. U.S.A.* 102, 9583–9588.
- Dong, R. P., Kameoka, J., Hegen, M., Tanaka, T., Xu, Y., Schlossman, S. F., and Morimoto, C. (1996) Characterization of adenosine deaminase binding to human CD26 on T cells and its biologic role in immune response, *J. Immunol.* 156, 1349–1355.
- Franco, R., Valenzuela, A., Lluís, C., and Blanco, J. (1998) Enzymatic and extraenzymatic role of ecto-adenosine deaminase in lymphocytes, *Immunol. Rev.* 161, 27–42.
- Kameoka, J., Tanaka, T., Nojima, Y., Schlossman, S. F., and Morimoto, C. (1993) Direct association of adenosine deaminase with a T cell activation antigen, CD26, *Science* 261, 466–469.
- Blanco, J., Marie, I., Callebaut, C., Jacotot, E., Krust, B., and Hovanessian, A. G. (1996) Specific binding of adenosine deaminase but not HIV-1 transactivator protein Tat to human CD26, *Exp. Cell Res.* 225, 102–111.
- Richard, E., Arredondo-Vega, F. X., Santisteban, I., Kelly, S. J., Patel, D. D., and Herschfield, M. S. (2000) The binding site of human adenosine deaminase for CD26/Dipeptidyl peptidase IV:

- the Arg142Gln mutation impairs binding to cd26 but does not cause immune deficiency, *J. Exp. Med.* 192, 1223–1236.
24. Schrader, W. P., West, C. A., Miczek, A. D., and Norton, E. K. (1990) Characterization of the adenosine deaminase-adenosine deaminase complexing protein binding reaction, *J. Biol. Chem.* 265, 19312–19318.
 25. Daddona, P. E., and Kelley, W. N. (1978) Adenosine deaminase: characteristics of the normal and mutant forms of the human enzyme, *Ciba Found. Symp.* 177–191.
 26. Weihofen, W. A., Liu, J., Reutter, W., Saenger, W., and Fan, H. (2004) Crystal structure of CD26/dipeptidyl-peptidase IV in complex with adenosine deaminase reveals a highly amphiphilic interface, *J. Biol. Chem.* 279, 43330–43335.
 27. Chien, C. H., Huang, L. H., Chou, C. Y., Chen, Y. S., Han, Y. S., Chang, G. G., Liang, P. H., and Chen, X. (2004) One site mutation disrupts dimer formation in human DPP-IV proteins, *J. Biol. Chem.* 279, 52338–52345.
 28. Chen, Y. S., Chien, C. H., Goparaju, C. M., Hsu, J. T., Liang, P. H., and Chen, X. (2004) Purification and characterization of human prolyl dipeptidase DPP8 in Sf9 insect cells, *Protein Expression Purif.* 35, 142–146.
 29. Sambrook, J., Fritsch, E. F., and Maniatis, T. (1989) *Molecular Cloning: A Laboratory Manual*, 2nd ed., Cold Spring Harbor Laboratory, Cold Spring Harbor, NY.
 30. Chang, H. C., and Chang, G. G. (2003) Involvement of single residue tryptophan 548 in the quaternary structural stability of pigeon cytosolic malic enzyme, *J. Biol. Chem.* 278, 23996–24002.
 31. Richard, E., Alam, S. M., Arredondo-Vega, F. X., Patel, D. D., and Hershfield, M. S. (2002) Clustered charged amino acids of human adenosine deaminase comprise a functional epitope for binding the adenosine deaminase complexing protein CD26/dipeptidyl peptidase IV, *J. Biol. Chem.* 277, 19720–19726.
 32. Daddona, P. E., and Kelley, W. N. (1978) Human adenosine deaminase binding protein. Assay, purification, and properties, *J. Biol. Chem.* 253, 4617–4623.
 33. Aertgeerts, K., Ye, S., Shi, L., Prasad, S. G., Witmer, D., Chi, E., Sang, B. C., Wijnands, R. A., Webb, D. R., and Swanson, R. V. (2004) N-linked glycosylation of dipeptidyl peptidase IV (CD26): effects on enzyme activity, homodimer formation, and adenosine deaminase binding, *Protein Sci.* 13, 145–154.

BI060401C